SCALING OF THERMAL DAMAGE OF CEMENTITIOUS MATERIALS

A.Menou[a,c], Gh. Mounajed[b], H. Boussa[b], Ch. La Borderie[c]

[a] AIMAC/ONDA Office National Des Aéroports du Maroc, Casablanca, Morocco
[b] CSTB/MOCAD, 84 Av Jean Jaurès, 77447 Marne la Vallée cedex 02 France
[c] LaSAGeC, ISA-BTP/UPPA, Allée du parc Montaury, 64600 Anglet, France

ABSTRACT

Within the framework of the study of concrete structures subjected to fire, a theoretical and experimental work has been achieved. The aim of this study is to investigate and to model the damage mechanisms of concrete after exposure to high temperature. The multiphase Digital Concrete Model and the damage model, MODEV, implemented on finite-element software SYMPHONIE, were used simultaneously to model the thermal damage of concrete exposed to high temperature. In order to validate the thermal damage model, an experimental investigation was carried out. The measurement of the mechanical characteristics of 5 cementitious materials, cement paste, mortar, ordinary concrete and 2 HPC concretes were performed by 3-point bending tests after heating/cooling cycles at 120, 250 and 400°C. The experimental tests on the 3 different cementitious materials compared to numerical simulation are presented for temperatures up to 400°C. After the validation of the models, several applications have been investigated, such as fire resistance of concretes.

Keywords: fracture energy, thermal damage, high temperature, concrete model, cement paste, micro-macro

1. Introduction

This research has been conducted within the framework of the study of concrete behaviour at high temperature. The experimental studies show an important influence the temperature on the behaviour of concretes, and in particular of High-Strength Concretes (HSC).

Several experimental research studies[1,2] have highlighted the complexity of the concrete behaviour when subjected to high temperature. This research work shows the existence of a combination of damage mechanisms of different origins: mechanical (strain), physical (heat transfer, free water transfer, variation of conductivity, etc.) and chemical (dehydration, carbonization, chemical transformations, etc.) [3].

In the theoretical model, we consider that the experimentally observed global damage is broken down into a thermal damage of mechanical origin due to non-free thermal strain (at macroscopic and microscopic level) on the one hand, and a thermal damage (not accompanied by strain) due to the physical- chemical transformations of the material, on the other hand.

In this research, we will use the microscopic multi-phase Digital-Concrete F.E. model (DC) [4], as well as the macroscopic deviatoric damage model MODEV to evaluate thermal damage at macroscopic and microscopic level. These two models are implemented in the general F.E. code SYMPHONIE [5]. The multi-scale approach allows a better understanding of the elementary mechanisms leading to the deterioration of the concrete with temperature; while highlighting the effect of the differential thermal expansion between cement paste and aggregates. Using the two previous models as a basis, a new approach to the thermal damage of concretes is presented

2. Multi-scale approach

2.1 Heterogeneous materials and limit of the macroscopic approach

The thermal damage of concrete presents a specific mechanism directly associated with the nature of this heterogeneous material. The analysis of the different macroscopic models shows the insufficiency of this approach regarding the representation of the complex mechanisms involved in the thermal damage.

Corresponding Author: E-Mail: abdellah.menou@univ-pau.fr

Courtesy: Proceedings of 2nd international conference on Recent Advances in Material Processing Technology-National Engineering College & Society for Manufacturing engineers, K. R. Nagar, Kovilpatti – 628 503, Tamilnadu, India

Some processes of degradation of this material are governed by several mechanisms which occur to a lesser extent.

2.2 New approach

In our approach, we have divided into two major categories the basic mechanisms that lead to the thermal damage of concrete.

1. Mechanical thermal damage due to restrained thermal strain on a macroscopic and microscopic scale: The original mechanical damage can be the temperature gradient or the boundary conditions, or even the geometric shape on a macroscopic scale, and the differential expansion between the cement paste and the aggregates on a microscopic scale

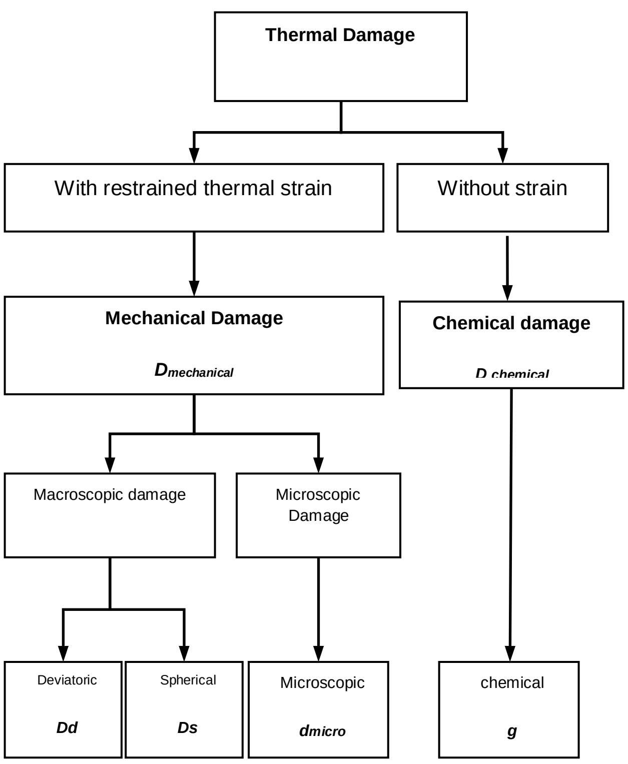

Fig. 1 . Thermal damage approach of concrete

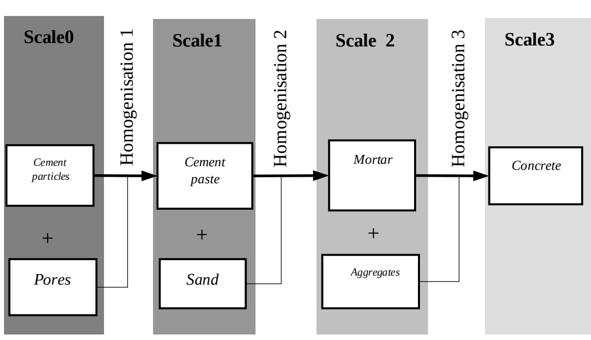

Fig. 2. Different phases for homogenization

2. Purely thermal damage due to the different chemical transformations, which occurs mainly in cement paste: dehydration, important mass loss beyond 120°C, and other chemical transformations.

2.3 Principle of the multi-scale identification of thermal damage

In this method, we consider several scales of modelling, ranging from the cement paste to the concrete material. Thus, the concrete is considered as a combination of three materials: cement, mortar, and concrete. Each material is considered on its specific scale, and homogenisation is needed on each scale to go to the following upper one. Fig. 2 shows the basis of this approach.

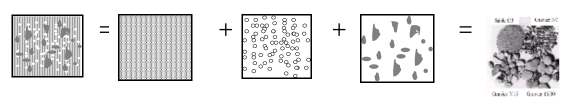

Fig. 1. Digital concrete model

The chemical damage in the cement paste, g, is the only part of the total damage that should be identified through experiments in our approach.

The mechanical and thermal characteristics of sand aggregates are conjointly injected into the Digital Concrete DC model with the evolution of the chemical damage in the cement in order to homogenize the mortar behaviour.

This process is continued with the homogenized mortar and concrete aggregates to finally obtain the thermo-mechanical concrete behaviour.

3. The basis of the models used

In this part, we present the basis of the Digital Concrete (DC) model and MODEV damage model implemented into SYMPHONIE F.E code and used simultaneously to identify the thermal damage of concrete.

3.1 The DC microscopic model

1st phase: Solid skeleton of the matrix cement P1

2nd phase: A random distribution of pores with the possibility of analyzing this phase in n subphases to represent different volumes and natures of pores P21, P22,… P2n

3rd phase: A spatial random distribution of aggregates with the possibility of analyzing this phase in m subphases to take into account the different sizes and different natures of aggregates P31,…, P3m.

3.2 The macroscopic damage model MODEV

MODEV is a new deviatoric damage model. This model is based on the damage mechanics approach and on the thermodynamics. This model uses a non-symmetrical criterion in strain.

By analogy with the equivalent Mazars strain[4], translating the local state of extension of a material, the model introduces two new equivalent strains translating respectively local sliding and crack opening. They are calculated respectively from deviatoric parts of the strain tensors and the spherical one. The MODEV model considers two scalar damage variables, corresponding respectively to each degradation mechanism. Each damage variable has its own evolution law.

$$\boldsymbol{\varepsilon} = \boldsymbol{\varepsilon}^d + \boldsymbol{\varepsilon}^s = \boldsymbol{\varepsilon}^d + \varepsilon^H \mathbf{I} \qquad (1)$$

$$f\left(\boldsymbol{\varepsilon}^s, K_s\right) = \tilde{\varepsilon}^s - K_s(D_s) = 0 \qquad (2)$$

$$f\left(\boldsymbol{\varepsilon}^d, K_d\right) = \tilde{\varepsilon}^d - K_d(D_d) = 0 \qquad (3)$$

$K_s(D)$ and $K_d(D)$are the evolution functions of spherical and deviatoric damages. The equivalent spherical strain $\tilde{\varepsilon}^s$ and the deviatoric equivalent strain $\tilde{\varepsilon}^d$ translating the local state of damage of the material are defined as follows:

$$\tilde{\varepsilon}^d = \sqrt{\left(\varepsilon_1^d\right)^2 + \left(\varepsilon_2^d\right)^2 + \left(\varepsilon_3^d\right)^2} + \alpha\varepsilon^H \qquad (4)$$

$$\tilde{\varepsilon}^s = \varepsilon^H \sqrt{3} \qquad (5)$$

where ε_i^d are the Eigen values of the deviatoric strain tensor;

α=0.35 is a coupling coefficient to take into account the hydrostatic effect.

The global macroscopic mechanical damage is deduced by combining the 2 damage variables:

$$(1 - D_{macro}) = (1 - D_s)(1 - D_d) \qquad (6)$$

4. STUDY OF THERMAL DAMAGE

4.1 Thermal damage due to restrained thermal strain

As described above, the thermal damage due to restrained thermal strain is broken down into macroscopic damage D_{macro} and microscopic damage d_{micro}. The global thermal damage is obtained by the following combination:

$$D_{mechanical} = 1 - \left(1 - D_{macro}\right)\left(1 - d_{micro}\right). \qquad (7)$$

Fig. 4 shows the DC simulated evolution of damage in a free concrete sample - whose size is 10 times the size of the coarser aggregate - at different temperatures.

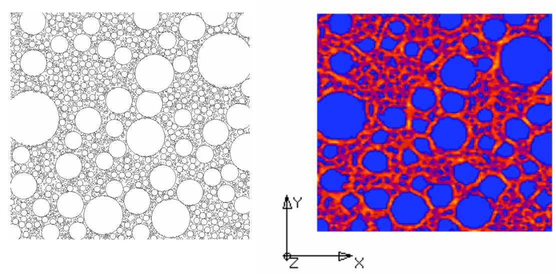

a) Aggregates generation Damage distribution at 150°C

Fig. 2. DC micromechanical damage with DC model (1)

4.2 Thermal damage due to physical/chemical transformations

This damage has been considered in the model by introducing the so-called *g* damage variable. The evolution of this variable is obtained directly from the experiment conducted on cement paste samples.

The damage variable *g* has been identified experimentally from a test performed on free cement samples [6]. Fig. 5 shows the g function, obtained by fitting experimental results, introduced into DC model.

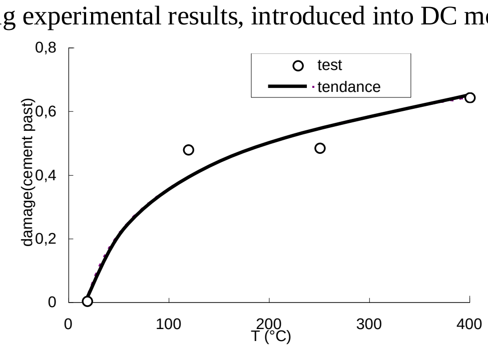

Fig. 3. Physical and chemical thermal damage origin

This function can be written as follows:

$$g(T) = 0.2 \cdot \mathrm{Ln}(T) - 0.6,\ g(T) \in [0,1[\qquad (8)$$

Finally, it results from this that the total damage can be written as follows:

$$1 - D = (1-d)(1-g) = \underbrace{\underbrace{(1-D_S)(1-D_d)}_{macro}\underbrace{(1-d_{micro})}_{dilatation}}_{1-d}\underbrace{(1-g)}_{\substack{chemical \\ 1-g}} \qquad (9)$$

5. Model validation

The validation of the model has been done by comparing experimental tests on cement mortar and concrete samples. The goal of this experimental study was threefold: to provide physical and chemical damage function *g*, to validate the numerical multi-scale homogenisation, and to evaluate the accuracy of this approach.

To do this, five materials were tested; cement paste, high-strength mortar (HSM), ordinary concrete (OC), and two types of high-strength concrete (HSC). All materials were tested on notched beam samples, previously heated according to the RILEM recommendations [8], subjected to three-point bending moments in order to get some fully steady tests. For each material, 3 notched beam samples 100x100x400 mm^3 were tested until failure. All samples were tested at 20°C after having undergone a heating cycle with the following temperatures: 20°C, 120°C, 250°C or 400°C. A temperature rate of 0.5°C/min was adopted for heating and cooling phases. The speed of heating and cooling was optimized by simulation in order to avoid any mechanical damage through the effect of the temperature gradient.

We assume that the chemical reactions and transformations will mainly take place in the cement paste (for temperatures ranging from 20°C to 400°C). After these simulations, we draw a comparison between numerically predicted laws and those obtained by experiments. The comparison that we present in this article applies to 3 of the 5 materials tested.

5.1 Mortar results

The test concerns a notched mortar beam sample, cut dimension (100x100x400 mm^3). The sample is slowly heated at a rate of 0.5°C/min until 400°C. For modelling this test with the DC model, we considered the mortar as a two-phase material: one phase of cement paste and n phases of sand aggregates defined according to the graduation of the material.

Fig. 4 shows the generation of the heterogeneous material with the DC model. The modelling of the temperature evolution is done by considering a transient thermal simulation with the applied boundary conditions on the body of the test sample (0.5°C/min).

Fig. 5 shows the iso-levels of the thermal damage at 400°C. Fig. 6 shows a comparison between experimental results and simulation. We can see the good capacity of the model for predicting the experimental test for the different levels of heating.

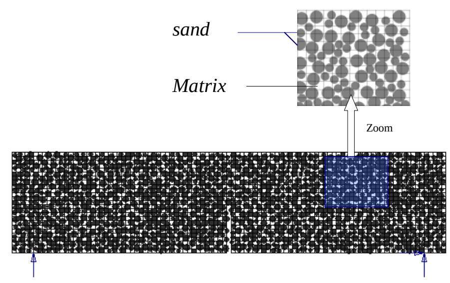

Fig. 4. Generation and boundary conditions (mortar)

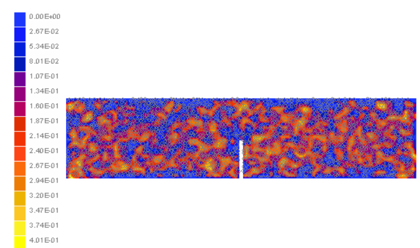

Fig. 5. Mortar thermal damage state with DC (Digital Concrete)

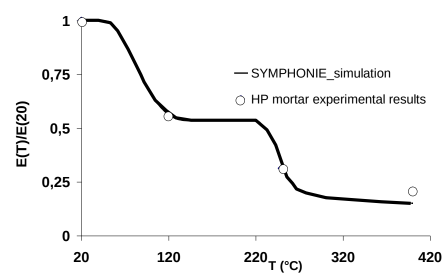

Fig. 6. Comparison between HSM experimental thermal damage and results of simulation

5.2 Results on Ordinary Concrete and High-Strength Concrete

As for mortar, the concrete test samples measuring (100x100x400 mm^3) were heated slowly at a rate of 0.5°C/min until 400°C. The tests were modelled with plain stress hypotheses while considering in this case, the concrete as a two-phase material: the homogenized mortar (made of cement paste and sand aggregates) and n phases of different size grading according to the composition of the material (Fig. 7).

The mechanical loadings were applied by prescribing displacements after thermal loading. The following figure shows the generation of the heterogeneous material with the DC model as well as the mechanical boundary conditions.

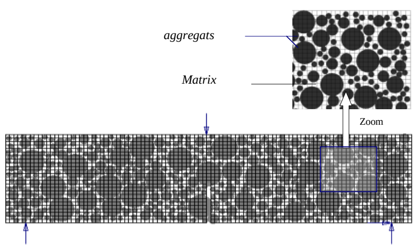

Fig. 7. Generation and boundary conditions(Concrete)

The results of simulation that we present here concern two different concretes:

Ordinary Concrete (OC) and High-Strength Concrete (HSC)

5.2.1 Ordinary Concrete results

Fig. 8 shows the experimental and simulated load-displacement curves of the OC at 250°C and 400°C.

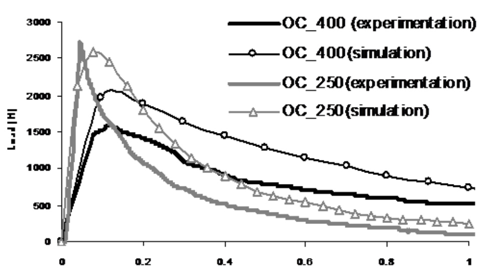

Fig. 8. Load-deflection at 250 and 400°C (OC)

Fig. 9 shows the ultimate loads at failure, obtained respectively by simulation and by tests according to the temperature. The comparison with the experimental results shows a good accuracy.

Fig. 10 shows the evolution of the fracture energy of the OC generated by simulation and compared to the experimental test at different temperature levels. We note that values of G_f obtained by simulation are very close to those given by tests.

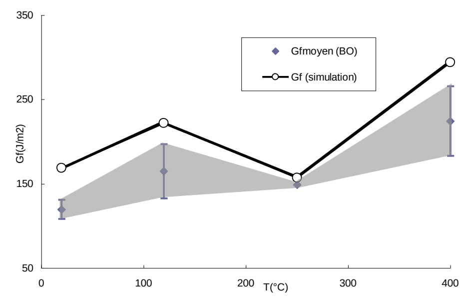

Fig. 9. Failure load Fmax simulation at high temperature (ordinary concrete)

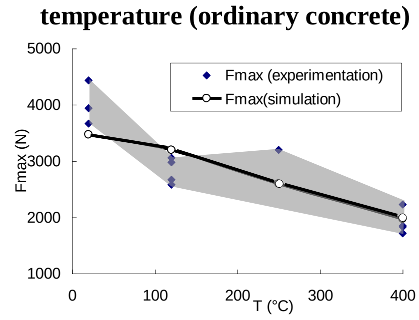

Fig. 10. Experimental evolution of the fracture energy Gf compared to the predicted evolution by simulation.

Fig. 11 shows the iso-levels of damage obtained by simulation on SYMPHONIE at 120°C and 400°C.

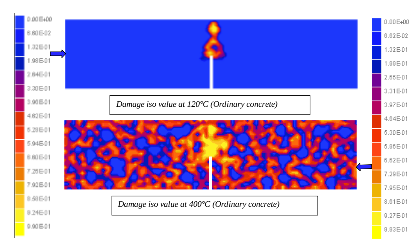

Fig. 11. Thermal damage iso-value at 120 and 400 °C (ordinary concrete)

5.2.2 High- strength concrete results

Fig. 12 shows the experimental and simulated load-displacement curves of the HSC at 250°C and 400°C.

Fig. 13 shows the experimental and predicted ultimate loads at failure for the different values of temperature.

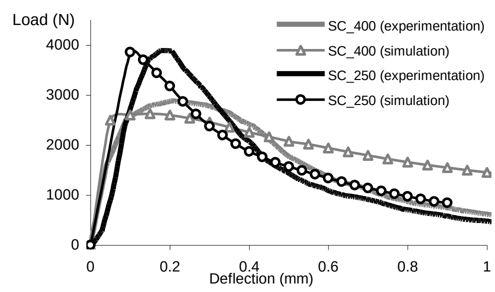

Fig. 12. Load-deflection at 250° and 400°C (HSC)

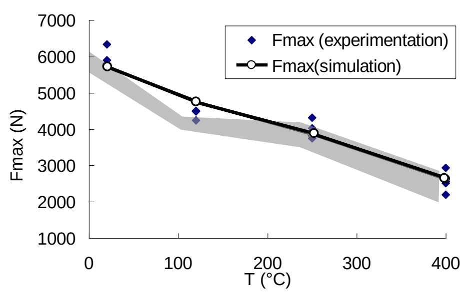

Fig. 13. Experimental and predicted values of ultimate loads at different temperature levels for HSC.

Fig. 14 shows a comparison between the experimental fracture energy and the simulated fracture energy as a function of temperature for HSC.

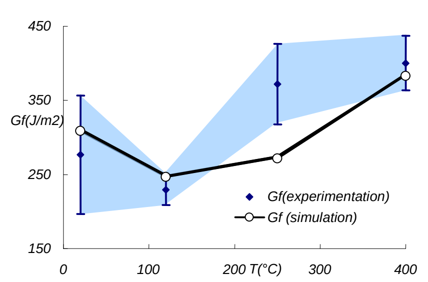

Fig. 14 . Predicted Fracture energy Gf by simulation and comparison with experimental results

6. Conclusion

A multi-scale simulation using a DC model was conducted on 4 cement-based materials: a High-Strength Mortar (HSM), an Ordinary Concrete (OC), a High-Strength Concrete (HSC)

A comparison between experimental results and simulation was presented. This comparison shows a good agreement between experiments and simulation for all of the tested materials.

These results confirm the relevance of the multi-scale approach to predict the total behaviour of cement-based materials and to quantify the thermal damage. This approach allows a better understanding of the original elementary mechanisms of the thermal damage evolution of concrete at high temperatures, and to clearly separate the mechanical damage (at micro and macro levels) from the physical/chemical damage. We can consider that the micro-mechanical damage of concrete mainly concerns the difference between the characteristics of the aggregates and the cement paste while the physical/chemical thermal damage mainly occurs in the cement paste.

References

[1] Bazant Zdenek P, Prat C. Effect of temperature and humidity on fracture energy of concrete.ACI Materials Journal. Technical paper Title no 85-M32. 1988.

[2] Baker G. 1996. The effect of exposure to elevated temperature on the fracture energy of plain concrete. Mater. & struct. 29(19): 383-388

[3] Diederichs U, Jumppanen U-M, Penttala, V. Behaviour of high-strength concrete at high temperatures. Helsinki University of Technology, Department of Structural Engineering, Report 92. 76 pages

[4] Lemaître J., Chaboche JL., 1988. Mécanique des matériaux solides. Dunod-1988

[5] Mounajed G, Hng Quoc H, Boussa H. Development of a new concrete damage model "MODEV" in SYMPHONIE F.E. code: Application to metallic anchor bolts. Poromechanics II, proceedings of the second BIOT conference on Poromechanics, (2002), Grenoble, France

[6] Mounajed G. 1991. SYMPHONIE, finit element software, CSTB, France. www.cstb.fr

[7] Mounajed G, Menou A, Boussa H, Pineaud A, Remond S, Cabrillac R. Comportement au feu des bétons. Approche multi échelles de l'endommagement thermique et identification expérimentale des paramètres. Revue Française de Génie Civil, Volume 7 – n°10/2003, pp 1299-1323

[8] RILEM – 1986. Détermination de l'énergie de rupture des mortiers et bétons par flexion trois points de poutres encochées. RILEM draft recommendationR. Plasticity induced crack closure under plane strain conditions in terms of dislocation arrangement. In: Lutjering